Applied Clay Science 157 (2018) 148–157

Contents lists available at ScienceDirect

Applied Clay Science

journal homepage: www.elsevier.com/locate/clay

Research paper

Influence of the synthetic conditions on the composition, morphology of CuMgAl hydrotalcites and their use as catalytic precursor in diesel soot combustion reactions

Nora Alejandra Comelli[a], María Lucía Ruiz[a], María Silvia Leguizamón Aparicio[b], Nora Andrea Merino[a], Juan Antonio Cecilia[c], Enrique Rodríguez-Castellón[c,*], Ileana Daniela Lick[b,*], Marta Isabel Ponzi[a]

[a] INTEQUI-CONICET-UNSL, 25 de Mayo 384, 5730 Villa Mercedes, San Luis, Argentina
[b] CINDECA (CCT) La Plata CONICET-UNLP, Departamento de Química, Facultad de Ciencias Exactas, Universidad Nacional de La Plata, Calle 47 N° 257, 1900 La Plata, Buenos Aires, Argentina
[c] Departamento de Química Inorgánica, Cristalografía y Mineralogía, Facultad de Ciencias, Universidad de Málaga, Campus de Teatinos, Málaga 29071, Spain

ARTICLE INFO

Keywords:
CuMgAl hydrotalcites
Soot combustion
Catalysis
Diesel

ABSTRACT

In this work, a series of Cu-Mg-Al hydrotalcites and the oxide mixture obtained by their calcination at 600 °C were synthesized by coprecipitation from metal nitrates. The effect of the coprecipitation temperature of the precursor on the structure and texture of these materials was investigated. The solids were characterised by inductively coupled plasma (ICP), atomic absorption spectrophotometry (AAS), an energy dispersive spectrometer (EDAX), thermogravimetric analysis (TGA-DTA), X-ray diffraction (XRD), scanning electron microscopy (SEM), X-ray photoelectron spectroscopy (XPS), and Fourier transform infrared spectroscopy (FTIR). It has been studied the activity of these solids as catalysts for diesel soot combustion. The materials are formed by nanoparticles, and the coprecipitation temperature has influence in the morphology of hydrotalcites. Moreover, the catalytic performance of calcinated solids is influenced by the synthesis conditions. A low temperature coprecipitation is beneficial for the diesel soot combustion. In this sense, the solid obtained by coprecipitacion at 40 °C shows the best catalytic activity (T_{max} = 375 °C). This catalyst contains cooper oxides, potassium and nitrate ions which can acts as promoters of the soot combustion. The studied solids showed activity and high resistance to the deactivation caused by hydro-treatment.

1. Introduction

The partial combustion that takes place in diesel engines leads to enormous emissions of pollutants as volatile organic compounds (VOCs), nitrogen oxides (NOx) and particulate matter (PM) (Van Setten et al., 2001). PM is a main constituent of air pollution, being associated to cardiovascular and respiratory diseases as well as skin cell alterations (Frank et al., 2013). PM is generally composed by elemental carbon (soot), soluble organic fraction (solid or liquid substances finely distributed in gases), sulfates (hydrated sulfuric acid, metal sulfates and liquid, depending on the sulfur content of the fuel) and ash (inorganic materials) (Guan et al., 2015). Soot particles can also be classified according to their aerodynamic diameter in large particles (> 10 μm), coarse particles (PM_{10}, 2.5–10 μm), fine particles ($PM_{2.5}$, 0.1–2.5 μm), ultra-fine particles ($PM_{0.1}$, 50–100 nm) and nanoparticles (< 50 nm), being reported that the smaller particles are the most harmful to human health (Prasad and Bella, 2011; Ristovsky et al., 2012).

The effect of the PM in the health and the environment has led to stringent environmental regulations for diesel emissions, being limited the PM emissions to 0.0021 g km^{-1} for light-duty vehicles and 0.01 g k Wh^{-1} for heavy-duty engine in the European Union (EU) and United States (US) (Johnson, 2014).

Diesel Particulate Filters (DPF) are sustainable processes to remove soot particles coming from the exhaust stream (Van Setten et al., 2001; Maricq, 2007). These filters are monoliths with channels in the form of honeycomb structure, where the soot particles get stuck. DPF are used as support to collect a metal-based catalyst to diminish the temperature of the soot combustion. Several active phases have been proposed to accelerate the soot combustion, such as noble metals catalysts mainly Pt (Oi-Uchisawa et al., 2000; Oi-Uchisawa et al., 2003), perovskite type oxide (Teraoka et al., 2001; Peng et al., 2007), spinel type oxides (Shangguan et al., 1998), rare earth metal oxides (Liu et al., 2005; Zhu

* Corresponding authors.
E-mail addresses: castellon@uma.es (E. Rodríguez-Castellón), ilick@quimica.unlp.edu.ar (I.D. Lick).

https://doi.org/10.1016/j.clay.2018.02.039
Received 28 October 2017; Received in revised form 15 February 2018; Accepted 26 February 2018

et al., 2005; Bueno-López, 2014).

In order to cheapen costs and to meet future expectation favoring Diesel engines, it is necessary the developing of inexpensive catalytic systems with higher performance and robustness to substitute the use of precious metals in soot combustion processes. In this sense, layered double hydroxides are inexpensive materials with potential to be used for the removal of the diesel soot particulate.

Layered double hydroxides, also denoted as hydrotalcites (HT), are classified as anionic clays, with general formula of:

$$[M(II)_{1-x}\, M(III)_x\, (OH)_2]\, (A^{m-})_{x/m} \cdot nH_2O]$$

where M(II) are divalent cations, M(III) are trivalent cations, A is an anion with charge m^-, and x is the M(III)/(M(III) + M(II)) molar ratio (Cavani et al., 1991; Vaccari, 1998 and Rives et al., 2001).

The intrinsic physicochemical properties of hydrotalcites present interesting applications as adsorbent (Nogueira et al., 2016), wastewater treatment (Aguiar et al., 2013), in separation processes (Kudinalli et al., 2015), ion exchanger (Lv et al., 2009) or polymer additives (Kalouskova et al., 2004). Moreover, the calcination of the layered double hydroxides leads to the formation of mixed oxides, which display interesting properties as heterogeneous catalyst (Rives et al., 2003; García-Sancho et al., 2011; Zhou et al., 2011; Alvarez et al., 2012; Helwani et al., 2013) or catalytic supports (Narayanan and Krishna, 2000) due to their large surface areas, basic character, high dispersion of the metal species. In addition, the presence of a transition metal cation in the chemical composition of the hydrotalcite can also provide redox properties for these solids. Several authors have evaluated the influence of variables such as pH and calcination temperature in the framework and the physicochemical behaviour of the hydrotalcites.

The most frequently synthesized hydrotalcite is the Mg-Al double hydroxide. Nonetheless, this hydrotalcite can be modified by cationic substitutions. In the present research have been incorporated Cu^{2+} species in the synthetic procedure. Previously, Rosales Suarez et al. (2007) evaluated the influence of the precipitating solution, pH, copper content, and mechanical milling on the structure and texture of hydrotalcites, finding that the pure hydrotalcite phase was obtained in all cases and that coprecipitation at pH 10. However, the use of large copper content causes changes in the cell parameters of the hydrotalcite increasing the values of the parameters "*a*" and "*c*", the crystallite size. Lwin et al. (2001) prepared a series of hydrotalcites by coprecipitation using metal nitrates as precursors and an aqueous solution of Na_2CO_3 as a precipitant agent, varying the Cu:Al atomic ratio between 0.5 and 4. These authors found that samples with very low Cu:Al ratio were amorphous, while an increase of the Cu:Al ratio led to the formation of malachite phase. Auer et al. (1999) prepared two series of Cu-Mg-Al hydrotalcites, one of them containing 33% Cu based on the total content of metals and another one with 67% Cu from their respective metal nitrates and with sodium carbonate as the precipitating agent, also obtaining malachite for the samples with higher copper content.

The use of hydrotalcite-based catalysts have received attention because they are rather stable materials that are able to deliver oxidizing species and promote diesel soot combustion and NO_x decomposition (Wang et al., 2007, 2012, 2014; Li et al., 2009a and Li et al., 2009b; Jiang et al., 2012; Comelli et al., 2013; Fino et al., 2016). The oxidizing capacity of diesel soot catalysts can be improved by the incorporation of copper or cobalt species (Sánchez et al., 2013; Jakubek et al., 2015).

The aim of the present research evaluates the influence of synthetic conditions of Cu-Mg-Al layered double hydroxides in their physicochemical properties as well as the textural properties of the mixed oxides obtained from the calcination of their respective hydrotalcite precursors at 600 °C. The obtained mixed oxides were tested in the diesel soot combustion reaction carrying out a detailed analysis of their resistance to the deactivation processes and the regeneration of the catalysts in successive catalytic cycles.

2. Experimental

2.1. Catalysts preparation

Hydrotalcites were synthesized by the co-precipitation method by mixing of an aqueous solution, solution A, which contain copper nitrate 0.66 M, ($Cu(NO_3)_2 \times 3H_2O$, Anedra), magnesium nitrate 0.66 M, ($Mg(NO_3)_2 \times 6H_2O$, Sigma-Aldrich) and aluminum nitrate 0.44 M ($Al(NO_3)_3 \times 9H_2O$,Sigma-Aldrich). In all cases, the atomic ratio between the divalent and trivalent cations in the solution was 3:1, while the Cu:Mg atomic ratio was 1:1. On the other hand, another aqueous solution (B) is prepared with the precipitating agents, i.e. potassium hydroxide 2 M (KOH, Cicarelli) and potassium carbonate 0.06 M ($K_2CO_3 \times 1.5H_2O$, Sigma-Aldrich). Later, solutions A and B were putted in different burettes and added dropwise into distilled water simultaneously, which was collected form a purification system in the laboratory, maintaining the pH between 9 and 10 under vigorous stirring at the chosen temperature (25 °C, 40 °C, 70 °C and 90 °C) and controlling the water evaporation. The samples were aged in the mother liquor maintaining the precipitation temperature for 3 h in the same beaker used for the reaction, covered with a glass lid. Then, the solids were filtered, washed several time with distilled water and dried at 110 °C for 12 h. In addition, an additional sample was synthesized by co-precipitation of their respective precursors at 40 °C, avoiding the washing step before the drying. The resulting solids exhibited different colours ranging from dark maroon to bluish green. Finally, the catalysts were obtained by calcining the precursor at 600 °C for 4 h.

The precursors were denoted as Pxyw or Pxynw, where *P* indicates the hydrotalcite precursor, *xy* indicates the coprecipitation temperature, *w* and *nw* indicate if the sample was washed or not washed, respectively. The catalysts were denoted as Cxyw or Cxynw, where *C* indicates that it is a calcined solid. All of the solids obtained were: P25w, P40w, P40nw, P70w, P90w, C25w, C40w, C40nw C70w and C90w.

2.2. Characterization of materials

The semiquantitative analysis and the surface morphology of the precursors and catalysts were performed with a scanning electronic microscope (SEM) LEO 1450 VP attached to an energy dispersive spectrometer (EDS) EDAX Genesis 2000, 20 Kv, with a working distance (WD) of 15 mm.

The elemental composition was determined by inductively coupled plasma optical emission spectroscopy (ICP-OES), with the use of a 1 m-Czemy Turner monochromator with a holographic grating with 1800 grooves mm^{-1}.

The temperature of the formation of the basic mixed oxides from hydrotalcites was determined by a TA-60 Shimadzu thermogravimetric (TG) and differential thermal analysis (DTA) instrument. In each experiment, 15 mg of hydrotalcite and α-Al_2O_3, as an inert reference material, were heated in Pt cups with a rate of 10 °C min^{-1}, from 20 °C to 700 °C, with a N_2 flow of 20 mL min^{-1}.

The crystalline structure of precursors and catalysts was studied by X-ray diffraction (XRD) using a D-Max III (Rigaku) with Cu Kα 1 radiation (λ = 1.5405 Å, 40 kV, 30 mA), with Ni filter, and scanning an angular range of 2θ between 10° and 70°, at a 3° min^{-1} rate.

Some samples were also studied by X-ray photoelectron spectroscopy (XPS) with a Physical Electronics PHI 5700 spectrometer with non-monochromatic Mg Kα radiation (300 W, 15 kV and 1253.6 eV) and a multi-channel detector. Spectra of samples were recorded in constant pass energy mode at 29.35 eV, using a 720 μm diameter analysis area. Charge was referenced against adventitious carbon (C 1*s* at 284.8 eV). A PHI ACCESS ESCA-V6.0 F software package was used for data acquisition and analysis. A Shirley-type background was subtracted from the signals. Recorded spectra were fit using Gaussian–Lorentzian curves in order to determine the binding energies

of the different element core levels more accurately. Prior the measurement, all samples were outgassed for 12 h prior to analysis under an ultra-high vacuum ($< 1.3 \times 10^{-6}$ Pa).

The presence of anions in the catalysts was studied using Fourier transform infrared spectroscopy (FTIR) with a Perkin-Elmer Spectrum RX1 instrument. The interferograms consisted of 80 scans, and the spectra were collected using a KBr spectrum as background. Spectra were recorded at room temperature in the 4000–400 cm^{-1} range. Discs were prepared with 70 mg of KBr and 5 mg of sample, using a pressure of 40 KN for 5 min.

2.3. Activity measurement

Two equipments were used to carry out catalytic experiments: a thermogravimetric reactor with an O_2/He feed and a fixed bed reactor fed with NO/O_2/He.

In the first case, the soot combustion was performed in a thermobalance (TG-60 Shimadzu) with a heating rate of 10 °C min^{-1} with mixture composed by air flow of 40 mL min^{-1} and N_2 flow of 20 mL min^{-1}. In order to carry out activity experiments, the soot (Printex-U, Degussa) and the catalyst were mixed in a 1/10 ratio, with an agate mortar (tight contact) before being introduced into the reactor. Mass loss and temperature were recorded as a function of time. The derivative curve (DTG) was obtained from the mass loss information as a function of time and from this curve the temperature which the combustion rate is maximum (T_{max}) was obtained. T_i and T_f are defined as the initial and final temperatures of the combustion process respectively, taken at the beginning and end of the derivative curve.

In the second case, to study the influence of the addition of NO_x on the catalytic behaviour, a fixed bed quartz microreactor (internal diameter = 0.8 cm) was used (Fig. 1). The reactor consists of a quartz tube in which the ceramic fiber used as catalyst bed is always placed in the same position. The total length of the reactor is 44 cm and is located in an electric furnace. The reaction mixture was obtained from three individually controlled lines: NO/He, O_2/He and He to balance. The mixture composition was 8% vol of O_2 and 1500 ppm of NO (total flow = 50 mL min^{-1}). The mixture soot/catalyst (1/10, w/w) loaded in the reactor was 33 mg. The temperature range studied was between 200 and 600 °C and the heating rate was 1.5 °C min^{-1}. Reaction products were analyzed with a gas chromatograph Shimadzu model GC-8A provided with a TCD detector. The separation of products was carried out in a CTRI concentric column (Altech). This system permitted identification and quantification of O_2, CO_2 and CO peaks. The amount of combusted soot was determined using the chromatographic information of CO_2 and CO (Ruiz et al., 2011).

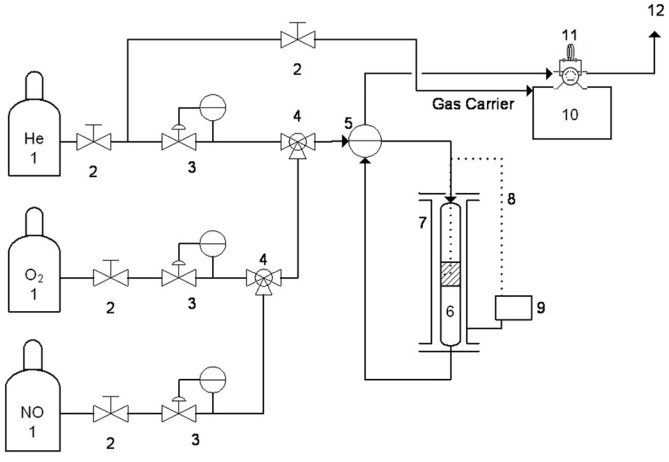

Fig. 1. Schematic diagram of the experimental set-up: unit (1), helium oxygen and nitric oxide cylinder; unit (2), On-off valves; unit (3), mass flow controllers; unit (4), Tee valves; unit (5), four-way valve; unit (6), quartz reactor; unit (7), furnace; unit (8), k type thermocouple; unit (9), thermostat; unit (10), gas chromatograph; unit (11), injection valve; unit (12), vent.

2.4. Deactivation by hydrotreatment

To study the behavior of the materials against hydrothermal treatments, catalysts were treated in water vapor presence at high temperature. Samples of catalysts were charged to a quartz fixed bed reactor fed with an inert gas stream (30 mL/min He) and this flow was saturated with water vapor (10% V/v). This ex-situ treatment was performed at 600 °C for 5 h. The hydro-treated samples were used in soot combustion experiments in a thermogravimetric reactor.

2.5. Reuse of the catalysts

The experiments of reuse of the catalysts were carried out in a thermogravimetric reactor. For this purpose used masses of catalysts were extracted from the reactor and then were intimately mixed with fresh soot (Printex-U) and the burning cycle was performed again. This operation was repeated four times (one with fresh catalyst and three reuses).

3. Results and discussion

The chemical composition of the synthesized hydrotalcites was analyzed by ICP. Taking into account that the theoretical molar ratio (Cu + Mg)/Al is equal to 3 and Cu/Mg ratio is 1, the chemical analysis carried out by ICP of the hydrotalcites show (Cu + Mg)/Al similar to the theoretical, while the Cu/Mg ratio are slightly higher than the nominal value. Several particles were analyzed by EDS to carry out a semiquantitative analysis of the hydrotalcites (Table 1). The EDAX results present a similar trend to those obtained by ICP, in the (Cu + Mg)/Al ratio and the Cu/Mg ratio, but with lower values. It is possible that these differences are due to scattered rays cannot leave the solid. Then, difference between EDS and ICP Cu/Mg ratio measurements can be associated to a Mg surface enrichment. Despite this, the EDS technique is easier to perform than other methods that require sample dissolution and successive dilutions.

The powder X-ray diffraction patterns of the precursors were carried out to determine their crystalline phases (Fig. 2). XRD profiles display diffraction peaks located at 2θ = 11.49, 23.19, 35.30, 39.70, 46.72, 61.40, 62.15 and 66.20°, which correspond to the presence of hydrotalcite (ICSD: 98-008-1963) (Cavani et al., 1991).

With regard to the synthetic conditions of the LDH, it has been reported in the literature the formation of a supercell with a Mg/Al = 3 M ratio, corresponding to the maximum observed substitution of magnesium by aluminum, Brindley and Kikkawa (1979) have reported that a M^{2+}/M^{3+} molar ratio higher than 2 can lead to the segregation of the M^{3+} cations. Cavani et al. (1991) also reported that the use of larger Mg/Al molar ratio leads to the segregation of aluminum species. In this sense, surface Mg/Al molar ratios obtained by EDS are smaller than

Table 1
Molar ratios obtained from ICP and EDS.

Solids	ICP		EDS	
	(Cu + Mg)/Al	Cu/Mg	(Cu + Mg)/Al	Cu/Mg
P25w	2.9	1.1	2.6	0.7
P40w	2.9	1.1	2.7	0.8
P70w	3.2	1.2	2.6	0.7
P90w	2.8	1.1	2.6	0.7
C25w	2.7	1.1	2.8	0.9
C40w	2.8	1.2	2.7	0.8
C70w	3.1	1.1	2.7	0.5
C90w	2.9	1.1	4.3	1.7

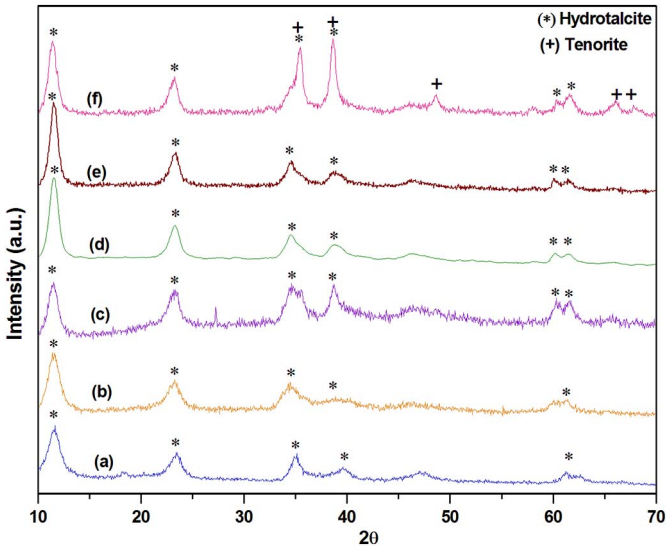

Fig. 2. XRD of the precursor: (a) HT; (b) P25w; (c) P40nw; (d) P40w; (e) P70w; (f) P90w.

those obtained by ICP. It is important to mention that no diffraction lines of segregated crystalline magnesium or aluminum species ($Mg(OH)_2$, Al_2O_3, MgO) are observed.

In the present work, it has been considered a molar ratio (Cu + Mg)/Al of 3. The ionic substitution Mg^{2+} by Cu^{2+} in the hydrotalcite should take place easily due to the similar ionic radii (Mg^{2+} = 0.073 nm and Cu^{2+} = 0.072 nm). The small shifts of the LDH peaks when copper species are added can be in agreement with the incorporation of copper species into the LDH framework. However, not all copper is incorporated into the network, part of it segregates and this fact also leads to the formation of new diffraction peaks located at 2θ = 32.44, 35.63, 39.17, 49.26, 58.41, 61.86, and 68.49° attributed to the presence of Cu species in the form of tenorite (CuO) (ICSD: 00-048-1548), which are more pronounced for the hydrotalcite synthesized at 90 °C, P90w. This sample contains CuO crystalline species and their crystal size, determined from the Debye-Scherrer equation, is 15 nm. An increase in the coprecipitation temperature leads to an increase in the relative intensity of the diffraction lines of the CuO with respect to those of the HT. Can be suggested that the introduction of Cu^{2+} species destabilizes the layered structure probably by the distorted octahedral coordination of the Cu ions by the Jahn -Teller effect and therefore the CuO can segregate. (Gao et al., 2012; Trujillano et al., 2006).

Previous research (Lwin et al., 2001; Auer et al., 1999) have reported the presence of malachite by the segregation of Cu-species in the synthesis of Cu-Mg-Al hydrotalcites for high Cu loadings; however these authors are not detected the presence of tenorite phase. Under this synthetic conditions, it should be expected the precipitation of the copper species in the form of hydroxide and/or hydroxyl carbonate species; however these species can evolve to more stable species such as oxides species (Cudennec and Lecerf, 2003), as indicates Fig. 2.

Table 2 compiles the crystalline size of the solids, determined from the Debye-Scherrer equation and the interlamelar distance, which was estimated by the Bragg Law, from the most intense diffraction line (d_{003}) in both cases.

An increase of the coprecipitation temperature leads to the formation of slightly larger LDH crystals. This fact is agreement with the literature where it is reported that precipitation at higher temperatures and longer aging times results in the formation of more ordered LDH-structures with larger crystal size. This result can be explained by taking into account the studies of Von Weimarn in the early twentieth century, which investigated the effects on the solubility (S) and concentration of the reactants (Q) on the average diameter of particles formed (d):

$$1/d = \text{constant}\ (Q - S)/S$$

Table 2
Structural parameters and chemical composition of the precursors.

Samples	FWHM[a]	t[b] nm	d[c] nm	Cu^{2+}:Mg^{2+}:Al^{3+} atomic ratio in solution in solid for ICP
MgAl	1.098	7.3	22.84	0.0:3.0:1.0 nd
P25w	1.092	7.3	22.84	1.5:1.5:1.0 1.5:1.4:1.0
P40nw	0.937	8.5	22.91	1.5:1.5:1.0 1.5:1.4:1.0
P40w	0.935	8.5	22.90	1.5:1.5:1.0 1.5:1.4:1.0
P70w	0.802	10.0	22.93	1.5:1.5:1.0 1.6:1.4:0.9
P90w	0.787	10.2	23.16	1.5:1.5:1.0 1.5:1.4:1.0

FWHM[a]: full width at half maximum (FWHM) of the (003) plane.
t[b]: crystallite size in the c direction calculated from the (003) plane using the Debye-Scherrer equation.
d[c]: interlayer spacing calculated using Bragg's law.
nd: not determined.

The (Q-S)/S ratio is the relative supersaturation (Skoog et al., 2015). The particle size is inversely proportional to the supersaturation. This condition is favored with increasing temperature because the solubility of copper nitrate, magnesium nitrate, and aluminum nitrate increases with increasing temperature. The interlayer distance also increases with increasing coprecipitation temperature, which is directly related to the increase in crystal size. The differences in structural parameters can be attributed to several factors: average charge of metal cations, the nature of the interlayer anion, coulombic attractive forces, water content and ionic species coordination (Sanchez-Cantu et al., 2010; Gao et al., 2012).

The scanning electron microscopy results obtained by SEM are shown in Fig. 3. The SEM micrographs reveal the existence of heterogeneous morphology. These particles are slightly larger when the coprecipitation temperature increases.

FTIR spectra of the LDH (Fig. 4) display a broad band between 3900 and 2700 cm^{-1} with a maximum about 3450–3500 cm^{-1}, which are assigned to the stretching mode of hydrogen-bonded hydroxyl groups (Rives and Kannan, 2000; Lopez et al., 1997; Nogueira et al., 2016). All spectra also show the presence of a band about 1640 cm^{-1}, which is characteristic of the water bending deformation located in the interlayer spacing and on the LDH surface (Lv et al., 2009; Nogueira et al., 2016). In addition, LDH display several bands between 700 and 1550 cm^{-1}, which are attributed to carbonate species located in the interlayer space (Nakamoto, 1997; Trujillano et al, 2009; Gondim et al., 2012). Finally, the band located about 2100 cm^{-1} is attributed to CO_2 adsorbed species. The sample non-washed, i.e. P40nW (curve b), displays similar profile than the other samples.

XPS analyses were performed using P40nw, P70w, C40nw and C70w samples, with the aim to obtain information about the chemical state and surface composition of the Cu-Mg-Al compounds. The ratio atomic concentrations at the surface were calculated from the peak areas considering photoelectron cross sections and mean free paths. C 1*s* core level spectra of P40nw and P70w exhibit two contributions located about 284.8 and 289.0 eV ascribed to the presence of adventitious carbon and carbonate species (Nogueira et al., 2016), respectively. The O 1*s* core level spectra display a band about 530.9 eV (García-Sancho et al., 2011), which is attributed to the coexistence of hydroxyl and carbonate species. The Al 2*p* core level spectra exhibit a contribution located about 74.1 eV, which is ascribed to the presence of aluminum hydroxide (Nogueira et al., 2016), while the Mg 2*p* core level spectra also show a contribution at 49.8 eV assigned to the existence of magnesium hydroxide (Guerrero-Urbaneja et al., 2014). Finally, Cu $2p_{3/2}$ core level spectra (Fig. 5) display two contributions; the first one located at 933.6 eV, which is assigned Cu^{2+} species in the form of CuO species and the other one about 942.3 eV, which is attributed to the *shake up* satellite, typical of divalent species. Previous research have reported that the ratio between the area of the satellite and the area of the main peak allows the determination of the reduced copper species.

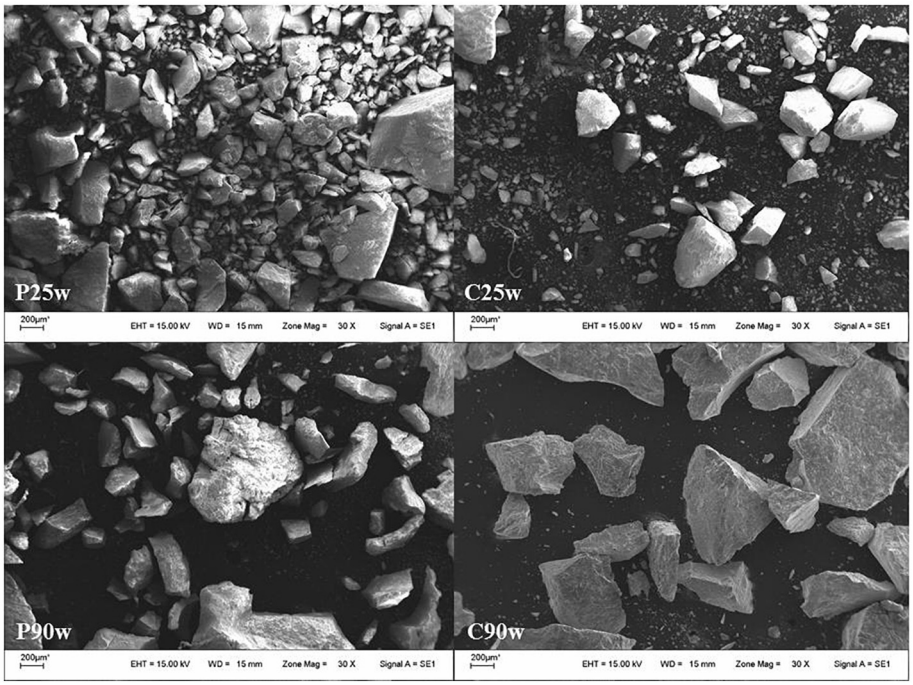

Fig. 3. SEM micrographs.

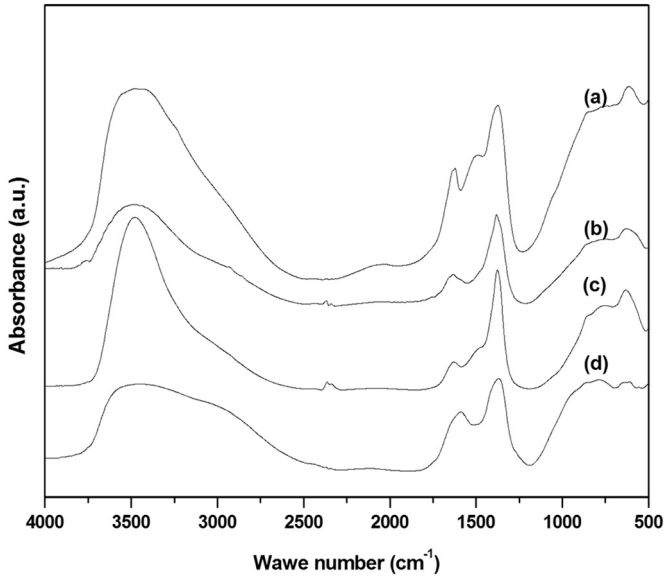

Fig. 4. FTIR spectra: (a) P25w; (b) P40nw; (c) P70w; (d) P90w.

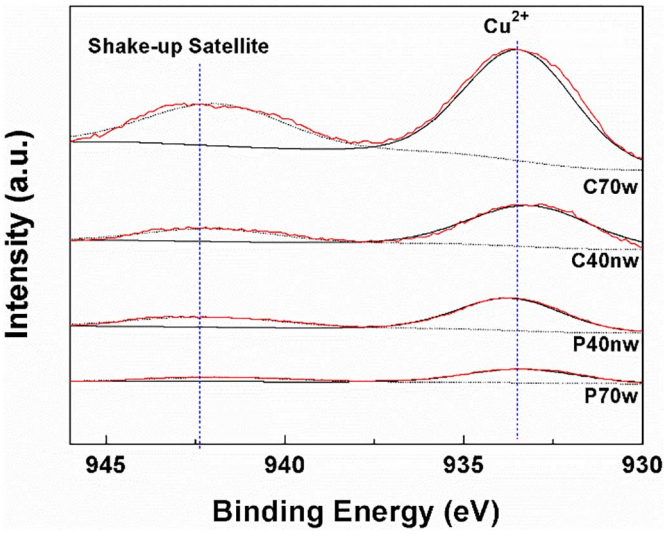

Fig. 5. Cu $2p_{3/2}$ core level spectra of hydrotalcites and calcined hydrotalcites.

Thus, it has been reported that pure CuO exhibits a I_{sat}/I_{mp} ratio of 0.55 (Avgouropoulos and Ionnides, 2003; Arango-Díaz et al., 2014). Data shown in Table 3 reveal that the I_{sat}/I_{mp} values are below than theoretical ones, which suggests the coexistence of Cu^{2+} and Cu^{+} species, although these species have not been detected by XRD. In this sense, previous research have pointed out that Cu species can be photoreduced so short irradiation time spectra were first registered to minimize the photoreduction of Cu^{2+} species. Nonetheless, a partial photoreduction is detected in all cases.

With regard to the atomic concentration on the surface of the catalytic precursors (Table 3), it can be observed how the $(Cu^{2+}+Mg^{2+})/Al^{3+}$ ratio is also below of the theoretical values ($M^{2+}/M^{3+}=3$) suggesting a higher proportion of aluminum species on the surface of the catalyst. These results are in agreement with results reported in the bibliography (Brindley and Kikkawa, 1979; Nogueira et al., 2016).

Table 3
XPS parameters of hydrotalcites and calcined hydrotalcites.

Sample	Atomic concentrations					Molar ratios		
	C 1*s*	O 1*s*	Mg 2*p*	Al 2*p*	Cu 2*p*	(Cu + Mg)/Al	Cu/Mg	I_{SAT}/I_{MP}
P40 nw	10.4	63.1	11.4	8.6	6.5	2.08	0.57	0.33
P70 w	11.3	63.6	11.2	8.1	5.9	2.10	0.52	0.35
C40 nw	12.8	57.1	11.0	14.6	4.4	1.05	0.40	0.31
C70w	15.3	55.6	9.9	13.6	5.3	1.08	0.56	0.37

However, there is a great variety of works in which the M^{2+}/M^{3+} ratio is modified. In any case, the hydrotalcite is formed and there are no segregations of oxides. The HT elemental formula presents a $M^{2+}/M^{3+}=2$ ratio, but some authors have established that with a relation $M^{2+}/M^{3+}=3$ a supercell is formed (Climent et al., 2004; Li et al., 2015).

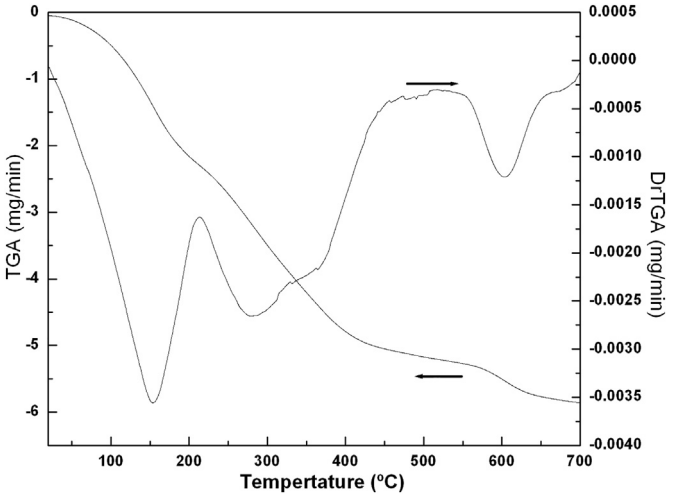

Fig. 6. TGA-DrTGA diagrams of P70w.

In the same way, the Cu/Mg ratio is far to the theoretical values too. The lower Cu/Mg molar ratio suggests that Cu species have low dispersion in comparison to the hydrotalcites, so it seems clear a phase segregation and the formation of crystalline structures with different particle size as was indicated from XRD previously.

The thermal decomposition of hydrotalcite was monitored for thermogravimetric analysis and was identified by mass spectroscopy for the P70W hydrotalcite and the evolution of the H_2O, NO, and CO_2 are shown in Fig. 6 and Fig. 7. The TGA/DTGA hydrotalcite can be decomposed in four stages with a total loss of 38% (Table 4). The first step, located between 20 and 192 °C, is attributed to the loss of physisorbed water molecules. In the next stages, the loss of H_2O, OH^-, and anions (CO_3^{2-}, NO_3^-), which are in the region of interlayer hydroxycarbonates, takes place (Trujillano et al., 2006). To avoid reactions in the gas phase between the decomposition products and molecular oxygen, the thermogravimetric analysis was carried out in an inert atmosphere. The mass losses obtained in an atmosphere containing oxygen are similar to those presented in Table 4.

The hydrotalcites were calcined at 600 °C were studied by XRD (Fig. 8). XRD profiles show how the use of lower coprecipitation temperature leads to broad diffraction peaks attributed to the presence of periclase (MgO) (43.08 and 62.55) (PDF N°: 98–006-0492) and tenorite (CuO). The use of higher coprecipitation temperature causes a rise of the diffraction peaks, which suggests an increase of the crystallinity. The CuO crystal size (Table 5) is higher in the samples that were obtained at higher coprecipitation temperatures. It cannot be detected diffraction peaks attributed to aluminum species, which suggests that these species should be amorphous or have small crystal size. It is evident the formation of oxidic phases, which come from the HT-like structures, and how the synthesis conditions have influenced on the crystallinity of the final oxidic phases, mainly in the CuO crystalline phases. It is important to mention that the C40nw sample exhibits very intense lines but the crystal size is similar than that found in the C40w sample, this fact suggest that the C40nw catalyst has a greater amount of detectable crystal species. In all the catalysts, probably a large amount of copper is present as CuO particles of very small size and high dispersion, which cannot be detected by XRD. This is explained as the coprecipitation temperature increases, the precipitation rate decreases, which lead to obtain segregated crystalline particles with a higher size. At lower temperatures, precipitation rate increases, and the solubility decreases, as a consequence more particles are obtained with smaller sizes.

SEM images, shown in Fig. 3, reveal that the calcined samples maintain an heterogeneous morphology. In addition, it is noticeable the increase of the particle size due to the decarbonation process that takes

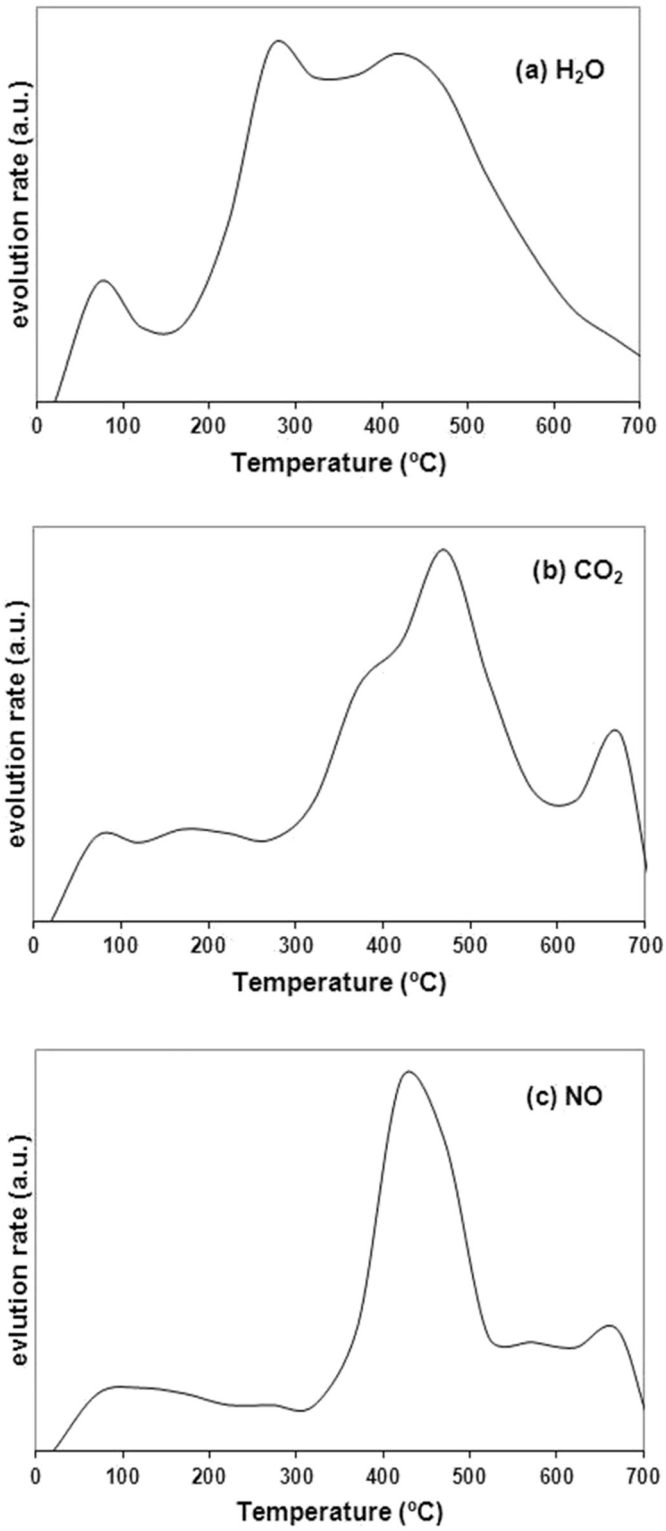

Fig. 7. Evolution of H_2O (a), CO_2 (b) and NO(c).

Table 4
Mass loss of P70w hydrotalcite.

Temperature range	% mass loss
RT-192	13.23
192–331	11.70
331–454	7.96
454–700	5.06

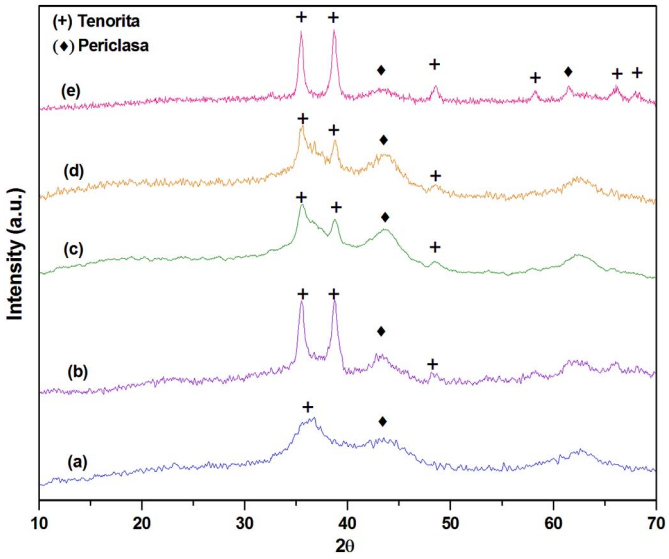

Fig. 8. XRD patterns of catalysts: (a) C25w; (b) C40nw; (c) C40w; (d) C70w; (e) C90w.

Table 5
Crystal size of CuO in catalysts.

Material	CuO crystal size (nm)
P40nw	13
P90w	15
C40nw	14
C40w	15
C70w	16
C90w	18

place during the calcination of hydrotalcite is an exothermic process (Correia et al., 2015).

The FTIR spectra of the calcined samples (Fig. 9) display a broad signal between 1330 and 1440 cm^{-1}. This signal could be ascribed to the presence of carbonate species probably due to the recarbonatation of the mixed-oxide species along the time (Correia et al., 2015). The presence of oxo-nitrogen species in the sample C40nw cannot be discarded since the absorption signal at 1385 cm^{-1} is very intense, in this zone, bands associated with the presence of nitrate species appear.

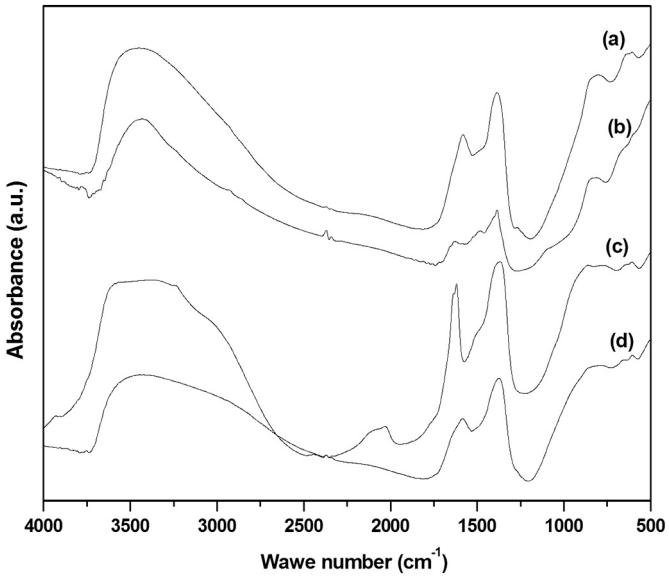

Fig. 9. FTIR spectra: (a) C25w, (b) C40nw, (c) C70w and (d) C90w.

The remainder potassium content in catalysts was determined by ICP and the results were 1%, 0.36%, 0.32%, 0.31% and 0.28% for C40nw, C40w, C25w, C70w, and C90w catalysts, respectively. When the precursor was intensively washed, potassium species are lost. Instead, the unwashed sample contains a high amount of potassium. This potassium can substantially promote the soot combustion. Several authors have reported that alkali metals increase the ability of the catalysts to adsorb and dissociate oxygen and also can form compounds with low melting point, which increase the contact between soot and catalyst (Feng et al., 2017; Carrascull et al., 2008).

The XPS of the calcined hydrotalcites (Table 3 and Fig. 5) do not show significant changes in the Mg 2*p*, Cu 2*p*, Al 2*p* core level spectra in comparison to their respective precursors. With regard to the C 1s region, it is noticeable how the contribution located about 289 eV, which is ascribed to carbonate species, decreases due to decarbonation by a thermal treatment of the hydrotalcites. Considering the calcination conditions, this contribution should disappear so the presence of carbonate species can be ascribed to a recarbonation of oxide MgO and CuO phases, confirming those shown in the FTIR spectra previously. In the same way, the O 1s region display a shift of its contribution to 531.2 eV, which is attributed to the presence of oxide species.

3.1. Catalytic results obtained using a thermogravimetric reactor

Results of soot conversion with the increase of temperature are shown in Fig. 11. Soot conversion was calculated according to Eq. (1).

$$\text{Soot Conversion (\%)} = \frac{(m - m_i)}{(m_i - m_f)} \times 100 \quad (1)$$

where m is variable mass, m_i is the mass at initial temperature (T_i) and m_f is the mass at final temperature (T_f).

The combustion temperature for a soot conversion of 50% (T_{50}), were 448, 490, 510, 515 and 525 °C for C40nw, C40w, C90w, C70w and C25w, respectively, meanwhile the T_{50} without catalyst was only of 610 °C. In previous research, (Comelli et al., 2013) observed a T_{50} soot conversion of 565 °C for MgO-Al_2O_3 catalysts obtained from the calcination of its respective hydrotalcite (curve f, Fig. 10) so it is clear that the presence of copper, as oxidic species, accelerates the combustion process. These results are in agreement with the bibliographical reports, indicating that the copper oxide species are promoters of the soot combustion due to its redox properties. (Aissat et al., 2010; Rico-Pérez et al., 2017; López-Suárez et al., 2014; Lick et al., 2008).

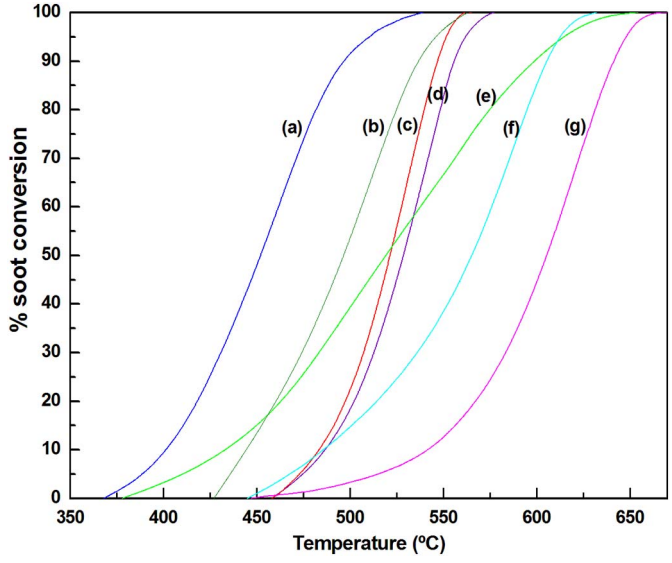

Fig. 10. Soot conversion: (a) C40nw; (b) C40w; (c) C70w; (d) C25w; (e) C90w; (f) MgAl; (g) soot without catalyst.

From catalytic data reported in Fig. 10, it can be observed that all catalysts follow similar trend, i.e. the soot combustion increases with the coprecipitation temperature of the hydrotalcite due to the formation of larger crystals, which implies a lower dispersion of the active site. In the case of the C90w, this trend is different. Thus, the onset reaction of this catalyst occurs close to the temperature of the most active catalyst, since C90w has more amount of CuO available on the surface as was indicated for the EDS results (Table 1). Nonetheless the complete conversion does not occur until high temperatures, which is attributed to the less amount of potassium and nitrate ions, according to the ICP and FTIR results. Moreover, these ions are more active than the CuO in the combustion process.

To study the influence of the washing treatment and the following calcination of the precursors, on the presence of nitrate species in the hydrotalcite-type catalysts, FTIR studies of C40nw and C40w catalysts were performed. When the precursor was intensely washed, the nitrate species were lost, since the intensity of the band at 1387 cm^{-1}, which is associated with the presence of nitrate ions, clearly decreased. The spectrum of the washed sample shows a signal around 1470–1520 cm^{-1}, which could be assigned to carbonate monodentate species originated because of the washing step. In the precursors of the catalysts higher nitrate content is also observed in the unwashed sample (Fig. 11).

The catalysts that showed higher activity were C40nw and C40w. Between both, the C40nw catalyst showed the lower combustion temperature, reaching a 100% conversion at 510 °C. The activity increase of this catalyst, which did not suffer the ion removal process by the washing stage of the synthesis is attributed to the presence of a higher content of potassium and nitrate ions, which can acts as promoters of the soot combustion (Aissat et al., 2010; Carrascull et al., 2003; Carrascull et al., 2008).

3.2. Catalytic results obtained using a fixed bed reactor

The results obtained in the soot combustion using a fixed bed reactor fed with a mixture of $NO/O_2/He$ are showed in Fig. 12. The catalysts presented in this study are able to decrease the soot combustion temperature following the next trend C40nw < C25w ≤ C70w < C90W under conditions near to reality of the performance of diesel motors.

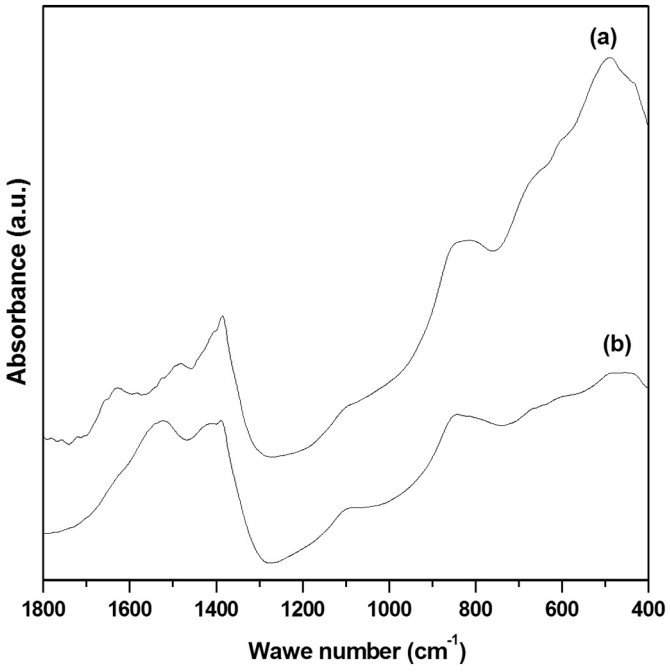

Fig. 11. FTIR spectra: (a) C40nw, (b) C40w.

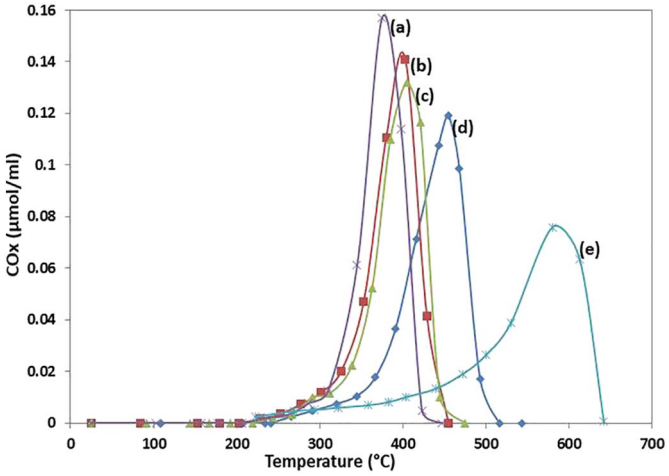

Fig. 12. Activity results obtained using a fixed bed reactor. (a) C40nw; (b) C25w; (c) C70w; (d) C90w; (e) soot without catalyst.

In spite of the presence of copper in the catalysts may improve the selectivity toward CO_2 formation and increase reducibility of nitrate ion (Lick et al., 2008), the activity was not clearly favored. Thus, the EDS data show how the activity and the copper content are not correlated.

The presence of nitrate ions, which is most evident in the catalyst prepared without the washing step (C40nw), are responsible for a good catalytic activity. Besides, the NO of the reaction flow can react with potassium species and generate “in-situ” superficial adsorbed oxo compounds of nitrogen, which can participate in the catalytic cycle. These nitrate ions participate in the soot combustion process, contributing with its redox cycle, nitrate/nitrite (Carrascull et al., 2003; Comelli et al., 2013; Ruiz et al., 2011; Aissat et al., 2010). It is evident that materials, prepared from hydrotalcite type precursors, exhibit good activity for the combustion of soot in the presence of NO_x. The T 50 values, required temperature to reach 50% of soot conversion, presented by the CuMgAl catalysts are very low and comparable with other reported catalytic results (Table 6).

3.3. Hydro-treatments effect on activity

The exhaust pipe of the engine operates at high temperature in water vapor presence, then one of the main disadvantages that may present catalysts for soot combustion is the deactivation by loss of the active species by dissolution. In this work the effect of the hydrotreatments on the activity of two catalysts, C40nw and C70w, was analyzed. These catalysts were chosen because the first one is the most active catalyst and the second one presents an intermediate activity. The results of the T_{ii}, shown in Table 7, indicate that the hydrotreatment slightly affects the activity of the C40nw sample and its Tmax shifted toward higher temperature (35 °C), this slight increase may be due to a leaching of the remaining potassium ions and/or nitrates

Table 6
Comparison of diesel soot combustion activity for different catalysts.

Catalyst	T 50	Reference
C40w	403	This work
C40nw	375	This work
$K/SrTiO_3$	450	López-Suárez et al. (2014)
$KCu/SrTiO_3$	490	López-Suárez et al. (2014)
$CuCeZrO_2$	490	Giménez-Mañogil and García-García, 2017
CuMgAlLa	391	Wang et al. (2014)
Mg Al La	430	Wang et al. (2014)
K HT based CoMgAlO	350	Li et al. (2009a, 2009b)
$Mn_{0.5}Mg_{2.5}CexAl_{1-x}O$	448	Li et al. (2014)

Table 7
Thermal and hydrothermal stability of catalysts.

	C40nw					C70w				
	Fresh	1°reuse	2°reuse	3°reuse	Hydrotreated	Fresh	1°reuse	2°reuse	3°reuse	Hydrotreated
Ti	359	414	403	380	359	450	422	419	422	450
Tmax	452	522	512	508	487	524	533	530	526	534

species. Thus, the catalytic behavior of the C70w catalyst is not substantially affected by hydrotreating, presenting a ΔT_{max} (fresh T_{max} – hydro-treated T_{max}) = 10 °C. The unwashed catalyst has high potassium content and NO_3^- active species available for the combustion reaction, and its exposure to a steam treatment causes that those species are solubilized more easily, a similar effect was observed by Ruiz et al. (2013).

3.4. Reuse of the catalysts

The reuse is a key factor in the sustainability of a catalyst. Thus, C40nw and C70w catalysts were evaluated in several combustion cycles. Table 7 shows T_i and T_{max}, of each reuse cycle. Both solids maintain the same trend, even after several runs. As was indicated for the fresh catalysts previously, the catalyst that was not washed during the synthesis presented the lower T_{max} (Table 3). The initial temperature (T_i) slightly increased for C40nw catalysts, in comparison with the one reached with the fresh catalyst. In contrast, the initial combustion temperature decreased for C70w catalysts. The T_{max} for both catalysts were higher in the reuses, but they decreased after each run. Analyzing these results, it can be concluded that the studied catalysts were slightly deactivated after the first use, but then they reached the stationary state and were not more deactivated when they were exposed to repeated cycles. This could be due to the regeneration and stability of nitrate species, being the C40nw performance similar to the one of the C40w fresh catalyst.

4. Conclusions

In this work it has been showed that the coprecipitation temperature does not have influence on the chemical composition, while it has influence in the morphology of hydrotalcites. Moreover, the catalytic performance that these solids have after being calcined is influenced by the synthesis conditions.

X-ray diffraction showed that pure hydrotalcite was obtained for all temperature range up to 70 °C; coprecipitation did show the presence of the malachite phase that is usually observed at high concentrations of Cu. When the temperature increased, the hydrotalcite had sharper signals, and the tenorite phase appeared 90 °C. Interlayer distance and crystallite size increased with increases in the coprecipitation temperature. For the hydrotalcites calcined at 600 °C, an increase in crystallinity with an increase in the coprecipitation temperature was also observed.

XPS results showed that the surface concentrations of Cu, Mg, O, and Al remained substantially constant. Cu was found on the surface of the hydrotalcite in the form of CuO.

The products of the thermal decomposition analyzed by a mass detector, for C70w catalyst, indicate that at 600 °C nitrates and carbonates have not been completely eliminated, which is in agreement with the results showed by the FTIR analyses.

A low temperature coprecipitation is beneficial to the diesel soot combustion. The C40nw solid showed the best catalytic activity (T_{max} = 375 °C), making suppose that the presence of potassium and nitrate ions would be the main responsible for this activity. Furthermore, the hydro-treatment slightly affects the activity of this catalyst.

Acknowledgment

Authors are thankful for the financial support of UNSL ("Universidad Nacional de San Luis" Project PROICO 14421), UNLP ("Universidad Nacional de La Plata" Project X707), ANPCYT (Project PICT 737) and CONICET (Project PIP 522), and Project CTQ2015-68951-C3-3-R from Ministerio de Economía y Competitividad of Spain and FEDER funds.

References

Aguiar, J.E., Bezerra, B.T.C., Braga, B.M., Lima, P.D.S., Nogueira, R.E.F.Q., de Lucena, S.M.P., da Silva, I.J., 2013. Adsorption of anionic and cationic dyes from aqueous solution on non-calcined Mg–Al layered double hydroxide: experimental and theoretical study. Sep. Sci. Technol. 48, 2307–2316.

Aissat, A., Siffert, S., Courcot, D., Cousin, R., Aboukaıs, A., 2010. VOCs and carbonaceous particles removal assisted by NOx on alkali $_{0.15}/ZrO_2$ and Csx–$M_{0.1}/ZrO_2$ catalysts (M = Cu or Co). C. R. Chimie 13, 515–526.

Alvarez, M.G., Chimentao, R.J., Figueras, F., Medina, F., 2012. Tunable basic and textural properties of hydrotalcite derived materials for transesterification of glycerol. Appl. Clay Sci. 58, 16–24.

Arango-Díaz, A., Cecilia, J.A., Moretti, E., Talon, A., Núñez, P., Marrero-Jerez, J., Jiménez-Jiménez, J., Jiménez-López, A., Rodríguez-Castellón, E., 2014. Comparative study of CuO supported on CeO_2, $Ce_{0.8}Zr_{0.2}O_2$ and $Ce_{0.8}Al_{0.2}O_2$ based catalysts in the CO-PROX reaction. Int. J. Hydrogen. Energ. 39, 4102–4109.

Auer, S.M., Gredig, S.V., Köppel, R., Baiker, A., 1999. Synthesis of methylamines from CO_2, H_2 and NH_3 over Cu–Mg–Al mixed oxides. J. Mol. Cat. A. Chemical. 141, 193–203.

Avgouropoulos, G., Ionnides, T., 2003. Selective CO oxidation over CuO-CeO_2 catalysts prepared via the urea-nitrate combustion method. Appl. Catal. A Gen. 244, 155–167.

Brindley, G.W., Kikkawa, S., 1979. A crystal-chemica study of Mg, Al and Ni, Al hydroxy-perchlorates and hydroxy-carbonates. Am. Mineral. 64, 836–843.

Bueno-López, A., 2014. Diesel soot combustion ceria catalysts. Appl. Catal. B Environ. 146, 1–11.

Carrascull, A., Lick, I.D., Ponzi, E.N., Ponzi, M.I., 2003. Catalytic combustion of soot with a O_2/NO mixture KNO_3/ZrO_2. Catal. Commun. 4, 124–128.

Carrascull, A., Lick, I.D., Ponzi, M., Ponzi, E.N., 2008. Diesel Soot combustion. KNO_3 and KOH supported on zirconia catalysts. React. Kinet. Catal. Lett. 94, 91–98.

Cavani, F., Trifiro, F., Vaccari, A., 1991. Hydrotalcite-type anionic clays: preparation, properties and applications. Catal. Today 11, 173–301.

Feng, N., Chen, C., Meng, J., Liu, G., Fang, F., Wang, L., Wan, H., 2017. K–Mn supported on three-dimensionally ordered macroporous La0.8Ce0.2FeO3 catalysts for the catalytic combustion of soot. Appl. Surf. Sci. 399, 114–122.

Climent, M.J., Corma, A., Iborra, S., Epping, K., Velty, A., 2004. Increasing the basicity and catalytic activity of hydrotalcites by different synthesis procedures. J. Catal. 225, 316–326.

Comelli, N.A., Ruiz, M.L., Merino, N.A., Lick, I.D., Rodríguez-Castellón, E., Jiménez-López, A., Ponzi, M.I., 2013. Preparation and characterization of calcined Mg/Al hydrotalcites impregnated with alkaline nitrate and their activities in the combustion of particulate matter. Appl. Clay Sci. 80–81, 426–432.

Correia, L.M., Campelo, N.S., Novaes, D.S., Cavalcante Jr., C.L., Cecilia, J.A., Rodríguez-Castellón, E., Vieira, R.S., 2015. Characterization and application of dolomite as catalytic precursor for canola and sunflower oils for biodiesel production. Chem. Eng. J. 269, 35–43.

Cudennec, Y., Lecerf, A., 2003. The transformation of $Cu(OH)_2$ into CuO, revisited. Solid State Sci. 5, 1471–1474.

Fino, D., Bensaid, S., Piumetti, M., Russo, N., 2016. A review on the catalytic combustion of soot in Diesel particulate filters for automotive applications: from powder catalysts to structured reactors. Appl. Catal. A Gen. 509, 75–96.

Frank, B., Schlögl, R., Su, D.S., 2013. Diesel soot toxification. Catal. Sci. Technol. 47, 3026–3027.

Gao, P., Li, F., Zhao, N., Wei, W., Zhong, L., Sun, Y., 2012. Effect of hydrotalcite-containing precursors on the performance of Cu/Zn/Al/Zr catalysts for CO2 hydrogenation: introduction of Cu^{2+} at different formation stages of precursors. Catal. Today 194, 9–15.

García-Sancho, C., Moreno-Tost, R., Mérida-Robles, J.M., Santamaría-González, J., Jiménez-López, A., Maireles-Torres, P., 2011. Etherification of glycerol to polyglycerols over MgAl mixed oxides. Catal. Today 167, 84–90.

Giménez-Mañogil, J., García-García, A., 2017. Identifying the nature of the copper entities over ceria-based supports to promote diesel soot combustion: synergistic effects.

Appl. Cata. A 542, 226–239.
Gondim, D., Lima, L., de Souza, M., Bresolin, I., Adriano, W., Azevedo, D.C.S., Silva Jr, I.J., 2012. Dye ligand epoxide chitosan/alginate: a potential new stationary phase for human IgG purification. Adsorpt. Sci. Technol. 30, 701–711.
Guan, B., Zhan, R., Lin, H., Huang, Z., 2015. Review of the state-of-the-art of exhaust particulate filter technology in internal combustion engines. J. Environ. Manege. 154, 225–258.
Guerrero-Urbaneja, P., García-Sancho, C., Moreno-Tost, R., Mérida-Robles, J., Santamaría-González, J., Jiménez-López, A., Maireles-Torres, P., 2014. Glycerol valorization by etherification to polyglycerols by using metal oxides derived from MgFe hydrotalcites. Appl. Catal. A Gen. 470, 199–207.
Helwani, Z., Aziz, N., Bakar, M.Z.A., Mukhtar, H., Kim, J., Othman, M.R., 2013. Conversion of Jatropha curcas oil into biodiesel using re-crystallized hydrotalcite. Energy Convers. Manag. 73, 128–134.
Jakubek, T., Kaspera, W., Legutko, P., Stelmachowski, P., Kotarba, A., 2015. Surface versus bulk alkali promotion of cobalt-oxide catalysts in soot oxidation. Catal. Commun. 71, 37–41.
Jiang, Z., Kong, L., Chu, Z., France, L.J., Xiao, T., Edwards, P.P., 2012. Catalytic combustion of propane over mixed oxides derived from CuxMg3–xAl hydrotalcites. Fuel 96, 257–263.
Johnson, T.V., 2014. Vehicular emissions in review. In: SAE Technical Paper, 2014-01-1491. https://doi.org/10.4271/2014-01-1491.
Kalouskova, R., Novotna, M., Vymazal, Z., 2004. Investigation of thermal stabilization of ply(vinyl chloride) by lead stearate and its combination with synthetic hydrotalcite. Polym. Degrad. Stab. 85, 903–909.
Kudinalli, L., Bhatta, G., Subramanyam, S., Chengala, M.D., Olivera, S., Venkatesh, K., 2015. Progress in hydrotalcite like compounds and metal-based oxides for CO_2 capture: a review. J. Clean. Prod. 103, 171–196.
Li, Q., Meng, M., Tsubaki, N., Li, X., Li, Z., Xie, Y., Hu, T., Zhang, J., 2009a. Performance of K-promoted hydrotalcite-derived CoMgAlO catalyst used for soot combustion, NOx storage and simultaneous soot-NOx removal. Appl. Catal. B Environ. 91, 406–415.
Li, Q., Meng, M., Zou, Z.Q., Li, X.G., Zha, Y.Q., 2009b. Simultaneous soot combustion and nitrogen oxide storage on potassium-promoted hydrotalcite-based CoMoAlO. J. Hazard. Mater. 161, 366–372.
Li, Q., Wang, X., Chang, W., Chen, H., Zhang, Z., 2014. Promotional effects of cerium doping and NOx on the catalytic soot combustion over MnMgAlO hydrotalcite-based mixed oxides. J. Rare Hearths 32, 176–183.
Li, Y., Bi, H.Y., Zhou, C.Y., 2015. Effects of Mg: Al molar ratio on the rheology of aqueous suspensions containing cationic starch and Mg/Al-hydrotalcite-like compounds. Russian Chem. Bull. Int Ed. 64, 2422–2426.
Lick, I.D., Carrascull, A.L., Ponzi, M.I., Ponzi, E.N., 2008. Zirconia-supported Cu-KNO_3 catalyst: characterization and catalytic behavior in the catalytic combustion of soot with a NO/O_2 mixture. Ind. Eng. Chem. Res. 47, 3834–3839.
Liu, J., Zhao, Z., Xu, C.M., Duan, A.J., Zhu, L., Wang, X.Z., 2005. Diesel soot oxidation over supported vanadium oxide and K-promoted vanadium oxide catalysts. Appl. Catal. B 61, 36–46.
Lopez, T., Bosch, P., Asomoza, M., Gómez, R., Ramos, E., 1997. DTA-TG and FTIR spectroscopies of sol-gel hydrotalcites: aluminum source effect on physicochemical properties. Mater. Lett. 31, 311–316.
López-Suárez, F.E., Bueno-López, A., Illán-Gómez, M.J., Trawczynski, J., 2014. Potassium-copper perovskite catalysts for mild temperature dieselsoot combustion. Appl. Catal. A 485, 214–221.
Lv, L., Sun, P., Gu, Z., Du, H., Pang, X., Tao, X., Xu, R., Xu, L., 2009. Removal of chloride ion from aqueous solution by ZnAl-NO_3 layered double hydroxides as anion-exchange. J. Hazard. Mater. 161, 1444–1449.
Lwin, Y., Ambar Yarmo, M., Yaakob, Z., Bakar Mohamad, A., Wan Daud, W.R., 2001. Synthesis and a characterization of Cu-Al layered double hydroxides. Mater. Res. Bull. 36, 193–198.
Maricq, M.M., 2007. Chemical characterization of particulate emissions from diesel engines: a review. J. Aerosol Sci. 38, 1079–1118.
Nakamoto, K., 1997. Infrared and Raman Spectra of Inorganic and Coordination Compounds. Wiley Interscience Publication, John Wiley and Sons, Inc., N.Y.
Narayanan, S., Krishna, K., 2000. Hydrotalcite-supported palladium catalysts: part II. Preparation, characterization of hydrotalcites and palladium hydrotalcites for CO chemisorption and phenol hydrogenation. Appl. Catal. A 198, 13–21.
Nogueira, K.A.B., Cecilia, J.A., Santos, S.O., Aguiar, J.E., Vilarrasa-García, E., Rodríguez-Castellón, E., Azevedo, D.C.S., Silva Jr., I.J., 2016. Adsorption behavior of bovine serum albumin on Zn-Al and Mg-Al layered double hydroxides. J. Sol-Gel Sci. Technol. 80, 748–758.
Oi-Uchisawa, J., Obuchi, A., Enomoto, R., Liu, S.T., Nanba, T., Kushiyana, S., 2000. Catalytic performance of Pt supported on various metal oxides in the oxidation of carbon black. Appl. Catal. B 26, 17–24.
Oi-Uchisawa, J., Wang, S.D., Nanba, T., Ohi, A., Obuchi, A., 2003. Improvement of Pt catalyst for soot oxidation using mixed oxide as a support. Appl. Catal. B 44, 207–215.
Peng, X., Lin, H., Shangguan, W., Huang, Z., 2007. A highly efficiente and porous catalyst for simultaneous removal of NO_x an diesel soot. Catal. Commun. 8, 157–161.
Prasad, R., Bella, R.V., 2011. Comparison of preparation methods of copper based PGM-free Diesel-soot oxidation catalysts. Bull. Chem. React. Eng. Catal. 6, 15–21.
Rico-Pérez, V., Aneggi, E., Trovarelli, A., 2017. The effect of Sr addition in Cu- and Fe-modified CeO_2 and ZrO_2 soot combustion. Catalysts 7, 28. http://dx.doi.org/10.3390/catal7010028.
Ristovsky, Z.D., Iljevic, B.M., Surawski, N.C., Moraska, L., Fong, K.M., Goh, F., Yang, I.A., 2012. Respiratory health effects of diesel particulate matter. Respirology 17, 201–212.
Rives, V., Kannan, S., 2000. Layered double hydroxides with the hydrotalcite-type structure containing Cu^{2+}, Ni^{2+} and Al^{3+}. J. Mater. Chem. 10, 489–495.
Rives, V., Dubey, A., Kannan, S., 2001. Synthesis, characterization and hydroxylation of phenol over CuCoAl ternary hydrotalcite. Phys. Chem. Chem. Phys. 3, 4826–4836.
Rives, V., Prieto, O., Dubey, A., Kannan, S., 2003. Synergistic effect in the hydrolation of phenol over CoNiAl ternary hydrotalcites. J. Catal. 220, 161–171.
Rosales Suarez, D., Zeifert, B.H., Hesiquio Garduño, M., Salmones Blasquez, J., Romero Serrano, A., 2007. Cu hydrotalcite-like compounds: morphological, structural and microstructural properties. J. Alloys Compd. 434–435, 783–787.
Ruiz, M.L., Lick, I.D., Ponzi, M.I., Rodriguez-Castellón, E., Jiménez-López, A., Ponzi, E.N., 2011. Combustion of diesel soot in NO/O_2 presence. Cesium nitrate and gold catalysts. Appl. Catal. A 392, 45–46.
Ruiz, M.L., Lick, I.D., Ponzi, M.I., Ponzi, E.N., 2013. Catalysts of alkaline nitrates supported on oxides for the diesel soot combustion. Deactivation by hydro-treatment and CO_2. Catal. Commun. 34, 45–51.
Sánchez, T., Gebretsadik, F.B., Salagre, P., Cesteros, Y., Guillén-Hurtado, N., García-García, A., Bueno-López, A., 2013. Evaluation of hectorites, synthesized in different conditions, as soot combustion catalysts after impregnation with copper. Appl. Clay Sci. 77, 40–45.
Sanchez-Cantu, M., Perez-Diaz, L., Maubert, A.M., Valente, J.S., 2010. Dependence of chemical composition of calcined hydrotalcite-like compounds. Catal. Today 150, 332–339.
Shangguan, W.F., Teraoka, Y., Kagawa, S., 1998. Promotioneffect of potassium on the catalytic property of $CuFe_2O_4$ for the simultaneous removal of NO_x and diesel soot particulate. Appl. Catal. B Environ. 16, 149–154.
Skoog, D.A., West, D.M., Holler, F.J., Crouch, S.R., 2015. Fundamentals of Analytical Chemistry, 9th edition. Cengage Learning Ed.
Teraoka, Y., Kanada, K., Kagawa, S., 2001. Synthesis of La-K-Mn-o perovskite-type oxides and theiir catalytic property for simultaneous removal of NO_x and diesel soot particualtes. Appl. Catal. B Environ. 34, 73–78.
Trujillano, R., Holgado, M.J., Pigazo, F., Rives, V., 2006. Preparation physicochemical characterization and magnetic properties of Cu-Al layered double hydroxides with CO_3^{-2} and anionic surfactants with different alkyl chains in the interlayer. Physica B 373, 267–273.
Trujillano, R., Holgado, M.J., Rives, V., 2009. Obtention of low oxidation states of copper from Cu 2þ–Al 3þ layered double hydroxides containing organic sulfonates in the interlayer. Solid State Sci. 11, 688–693.
Vaccari, A., 1998. Preparation and catalytic properties of cationic and anionic clays. Catal. Today 41, 53–71.
Van Setten, B.A.A.L., Makkee, M., Moulijn, J.A., 2001. Science and technology of catalytic diesel particulate filters. Catal. Rev. 43, 489–564.
Wang, Z., Jiang, Z., Shangguan, W., 2007. Simultaneous catalytic removal of NOx and soot particulate over Co–Al mixed oxide catalysts derived from hydrotalcites. Catal. Commun. 8, 1659–1664.
Wang, Z., Li, Q., Wang, L., Shangguan, W., 2012. Simultaneous catalytic removal of NO_x and soot particulates over CuMgAl hydrotalcites derived mixed metal oxides. Appl. Clay Sci. 55, 125–130.
Wang, Z., Zhang, Z. Yan X., Bi, X., Wang, L., Zhang, Z., Jiang, Z., Xiao, T., Umar, A., Wang, Q., 2014. Lanthanum-promoted copper-based hydrotalcites derived mixed oxides for NOx adsorption, soot combustion and simultaneous NOx-soot removal. Mater. Res. Bull. 51, 119–127.
Zhou, S., Qian, Z., Sun, T., Xu, J., Xia, C., 2011. Catalytic wet peroxide oxidation of phenol over Cu-Ni-Al hydrotalcite. Appl. Clay Sci. 53, 627–633.
Zhu, L., Wang, Z.X., Yu, J.J., Hao, Z.P., 2005. Catalytic performance of K-$Ce_{0.5}Zr_{0.5}O_2$ catalysts for soot combustion. Acta Phys. -Chim. Sin. 21, 80–845.